DOI: 10.1002/chem.200801301

Probing the Surface of Organic and Bioconjugated Nanocrystals by Using Mass Spectrometric Imaging

Hyegeun Min,[a, b] Yongwook Kim,[c] Hyunung Yu,[a, b] Dae Won Moon,[a, b] Sung Jun Lim,[c] Hye-Joo Yoon,[c] Tae Geol Lee,*[a, b] and Seung Koo Shin*[c]

The conjugation of water-soluble ligands on semiconductor nanocrystals is of practical importance in fluorescence tagging of biomolecules for in vivo and in vitro studies.[1] Fluorescent nanocrystals are typically synthesized in organic solvents, and then converted into water-soluble forms for the conjugation with biomolecules through covalent linkage or electrostatic interactions.[1] However, probing the surface of water-soluble and bioconjugated nanocrystals has become a challenge because of the heterogeneity of surface functional groups. To date, a number of attempts have been made to characterize chemical species conjugated onto nanocrystals: NMR and optical spectroscopy were used to validate the exchange of organic layers with dithiocarbamate moieties,[2] and FT-IR spectroscopy was employed to monitor the progress of ligand exchange and bioconjugation processes.[3] Nonetheless, these macroscopic analyses were unble to differentiate the surface ligands from other chemical species also present in solution. Recently, time-of-flight secondary-ion mass spectrometry (TOF-SIMS) has emerged as a promising tool capable of label-free analysis of surface ligands, ranging from small peptides conjugated on a single polystyrene bead in sizes of 30–60 μm to organic/biomolecules on biochips, at high spatial resolution (50–100 nm).[4]

In this report, we utilized the TOF-SIMS imaging to characterize surface ligands conjugated onto nanocrystals in sizes of 6–12 nm. When nanocrystals were placed on a matrix-free substrate, they formed aggregates spontaneously. The ion beam sputtering gave rise to the ionic signatures, not only of nanocrystals and surface ligands, but also of the substrate and other adsorbates. TOF-SIMS images displayed the micronscale pattern of nanocrystal aggregates separable from the substrate pattern. Thus, the surface ligands on nanocrystals were differentiated from other residues on the substrate.

The semiconductor nanocrystals used in this work, CdSe/ZnS(3ML) (ML = monolayer) with an average size of 5.6 ± 0.4 nm emitting at 640 nm, were prepared by trioctylphosphine oxide (TOPO)-free colloidal syntheses[5] (see Figure S1 in Supporting Information for high-resolution transmission electron microscopy images). In brief, CdSe nanocrystals were synthesized from reactions of CdO, stearic acid, and selenium powder in 1-octadecene (ODE) with octylamine as a growth additive. Three monolayers (MLs) of the ZnS shell were grown over the CdSe core through reactions of ZnO, oleic acid, and sulfur powder in ODE with octadecylamine (ODA) as an additive. Three different bifunctional hydrophilic thiols, 3-mercaptopropionic acid (MPA), 3-mercapto-1-propanol (MPO), and 2-aminoethane thiol (AET), were used to convert organic-soluble nanocrystals into water-soluble ones by ligand exchange (Scheme 1A→B). The hydrodynamic size was 12.2 ± 2.0,

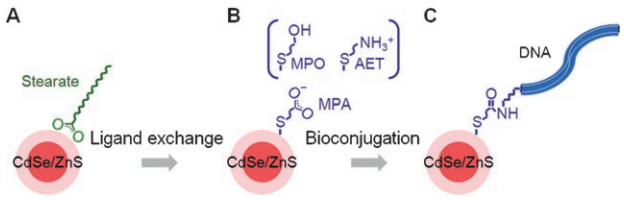

Scheme 1. Preparation of organic-soluble (A), water-soluble (B), and DNA-conjugated (C) CdSe/ZnS core/shell nanocrystals.

[a] H. Min, Dr. H. Yu, Dr. D. W. Moon, Dr. T. G. Lee
Nanobio Fusion Research Center
Korea Research Institute of Science and Standard
Daejeon 305-600 (Korea)
Fax: (+82) 42-868-5032
E-mail: tglee@kriss.re.kr

[b] H. Min, Dr. H. Yu, Dr. D. W. Moon, Dr. T. G. Lee
Department of Nano Surface Science
University of Science and Technology
Daejeon 305-333 (Korea)

[c] Y. Kim, S. J. Lim, Dr. H.-J. Yoon, Prof. S. K. Shin
Bio-Nanotechnology Center
Department of Chemistry
Pohang University of Science and Technology
Pohang, Kyungbuk 790-784 (Korea)
Fax: (+82) 54-279-3399
E-mail: skshin@postech.ac.kr

Supporting information for this article is available on the WWW under http://dx.doi.org/10.1002/chem.200801301.

11.7±2.4, and 10.2±1.9 nm for MPA-, MPO-, and AET-capped nanocrystal, respectively. DNA-conjugated nanocrystals were obtained by cross-linking thrombin-binding aptamer DNA to MPA-capped nanocrystals (Scheme 1B→C).

For TOF-SIMS analysis, nanocrystals were dropped onto a Si(100) substrate precleaned in a piranha solution and dried under vacuum. Most TOF-SIMS spectra were taken in the negative mode. A matrix-free substrate allowed the detection of secondary ions in a low mass region with high sensitivity.

Firstly, we obtained the IR spectra of organic-soluble and MPA-capped nanocrystals (Figure 1). NMR analysis was not carried out because of the limited amount of samples. Organic-soluble nanocrystals provide the IR fingerprints of stearic acid: strong C–H bands

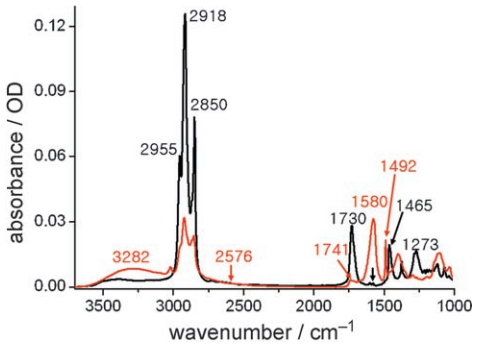

Figure 1. FT-IR spectra of organic-soluble (black) and MPA-capped water-soluble (red) nanocrystals.

and a C=O stretching band at 1730 cm^{-1} blue-shifted from 1697 cm^{-1} of free stearic acid, indicating hydrogen bonding between COOH groups.[6] On the other hand, MPA-capped nanocrystals display a broad O–H band at 3282 cm^{-1}, C=O stretching at 1741 cm^{-1}, and asymmetric and symmetric stretching of the uncoordinated COO$^-$ group at 1580 and 1492 cm^{-1}.[6] Although the IR spectra identify a number of functional groups, it remains unclear whether those functional groups are from the ligands conjugated onto the surface of nanocrystals or not.

Next, we obtained the micropattern of nanocrystals with TOF-SIMS at a spatial resolution of 1.5 μm. Figure 2a–d

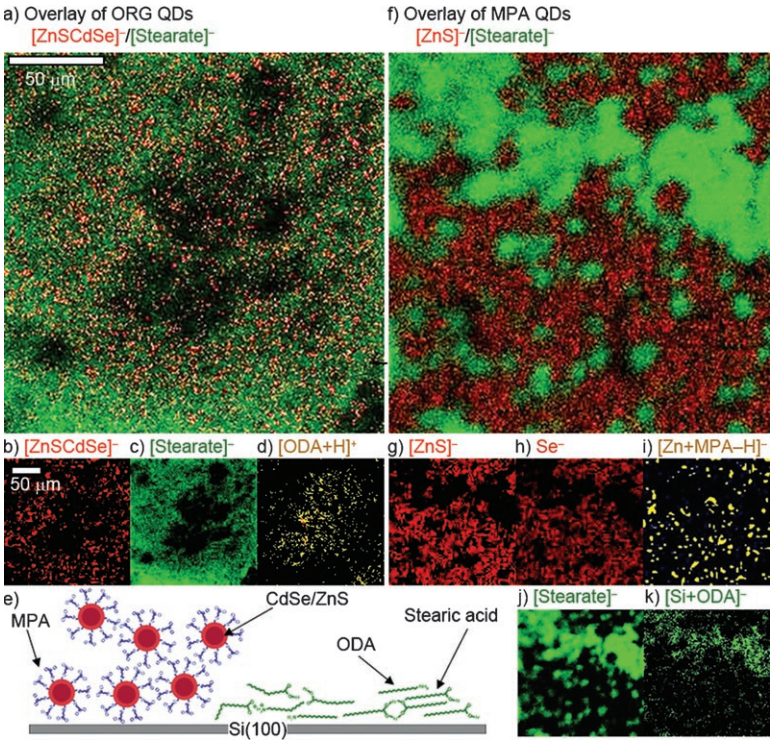

Figure 2. TOF-SIMS images of organic-soluble (ORG) (a–d) and MPA-capped water-soluble (MPA) nanocrystal quantum dots (QDs) (f–k); a) overlay of b) and c); b) [ZnSCdSe]$^-$; c) [stearate]$^-$; d) [ODA+H]$^+$, e) a schematic of MPA-capped nanocrystals on a Si substrate; f) overlay of g) and j); g) [ZnS]$^-$; h) Se$^-$; i) [Zn+MPA–H]$^-$; j) [stearate]$^-$; k) [Si+ODA]$^-$.

present organic-soluble nanocrystals. The image of [ZnSCdSe]$^-$ depicts the pattern of CdSe/ZnS nanocrystal aggregates formed on the substrate. Of the several organic compounds used in synthesis, stearate produces the most prominent peak at $m/z=283$. Although stearic acid was used in the CdSe core synthesis and oleic acid was employed in the ZnS shell synthesis, only stearate was observed in the mass spectra. Oleic acid might have been completely washed out during purification. The pattern of [stearate]$^-$ perfectly overlaps with that of [ZnSCdSe]$^-$, suggesting the presence of stearate on the surface of nanocrystals. In contrast, the [ODA+H]$^+$ image obtained in the positive mode shows a pattern absent of both nanocrystal and stearate, indicating that ODA is not on nanocrystals.

Figure 2f–k show MPA-capped water-soluble nanocrystals. Both [ZnS]$^-$ and Se$^-$ images display the micropattern of nanocrystals. The pattern of [Zn+MPA–H]$^-$ overlaps well with that of nanocrystals, confirming the ligation of MPA on the surface of CdSe/ZnS nanocrystals. Unlike organic-soluble nanocrystals, however, the pattern of [stearate]$^-$ does not overlap with that of nanocrystals, but with the [Si+ODA]$^-$ image, illustrating that both stearate and ODA are on the substrate. This comes as a surprise, because water-soluble nanocrystals were washed three times with ethyl acetate to remove residual organic compounds.

While the TOF-SIMS images show the ligation of MPA on the surface of nanocrystals, they lack information about the mode of binding. In contrast, the IR spectra identify the

functional groups, but they do not tell us the ligand specificity. By taking both data into account, we propose a scheme (Figure 2e) for the formation of MPA-capped nanocrystal aggregates on the silicon substrate. The appearance of $[Zn+MPA-H]^-$ in the mass spectra and the absence of an S–H stretching band in the IR spectra demonstrate the zinc–thiolate linkage between MPA and CdSe/ZnS nanocrystals. The IR signature of COOH hydrogen bonding (1741 cm^{-1}) suggests that MPA-capped nanocrystals are clustered together through hydrogen bonding between neighboring surface carboxyl terminal groups of adjacent nanocrystals. The overlapping images of $[stearate]^-$ and $[Si+ODA]^-$ occupying a nanocrystal-free space, as well as the uncoordinated COO^- stretching bands in the IR spectra, imply the coexistence of stearate and ODA on the substrate.

For MPO- and AET-capped nanocrystals, images of $[MPO-H]^-$ and $[AET-H]^-$ ions overlap with the $[ZnS]^-$ image representing nanocrystals, whereas the $[stearate]^-$ image does not (see Figures S2 and S3 in Supporting Information). Like MPA-capped nanocrystals, both MPO and AET are thus coordinated on the surface of CdSe/ZnS nanocrystals.

Finally, we obtained the TOF-SIMS image of DNA-conjugated nanocrystals. Figure 3 shows the TOF-SIMS spectra. $[PO_3]^-$, $[PO_2]^-$, Se^-, and $[Stearate]^-$ peaks appear strong. Of

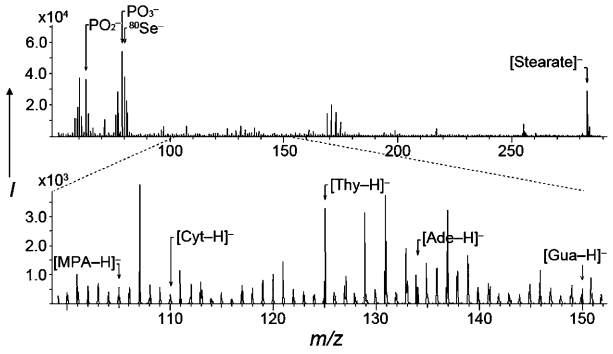

Figure 3. TOF-SIMS spectra of DNA-conjugated water-soluble nanocrystals.

the DNA fragment ions, $[Thy-H]^-$ appears most intense. For DNA, the base fragment ions are typically found in the low mass region and they stand out well above the noise level (see Figure S4 in the Supporting Information). However, the relative abundance of $[Base-H]^-$ barely correlates with the base composition of DNA.[7] Figure 4a–d display images of $[PO_3]^-$, $[Thy-H]^-$, $^{80}Se^-$, and $[stearate]^-$. The $[Thy-H]^-$ and $[PO_3]^-$ images are identical and images of DNA fragment ions overlap well with the Se^- image, confirming a spatial pattern of nanocrystal aggregates on the substrate. On the other hand, the image of $[stearate]^-$ does not overlap with that of nanocrystals. These contrasting images validate the conjugation of DNA onto the nanocrystals.

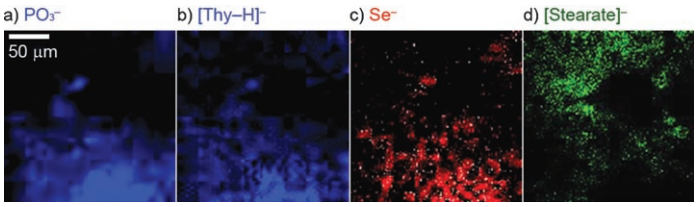

Figure 4. TOF-SIMS images of DNA-conjugated water-soluble nanocrystals. Each image represents DNA (a and b), nanocrystal (c), and stearic acid (d).

Interestingly, although both stearic and oleic acids are used in preparing metal precursors, only stearate is detected from all water-soluble nanocrystals. It is known that stearate forms micelles in water more easily than oleate.[8] Thus, it seems only stearate is transferred from the organic layer to water by forming water-soluble micelles during water-soluble ligand exchange processes and survived the washing steps. Thus, we think that unsaturated fatty acids like oleic acid are better than saturated ones like strearic acid for preparing metal precursors.

In summary, the TOF-SIMS imaging unequivocally proves whether or not organic ligands and biomolecules are conjugated on semiconductor nanocrystals in sizes of 6–12 nm. Nanocrystals display the micronscale pattern due to the self-aggregation during the vacuum drying process. The ligands conjugated on the surface show the patterns perfectly overlapping with those of nanocrystals. In contrast, other residual species present different spatial patterns. The multiplexed mass-fingerprint imaging is well suited to the surface analysis of various nanoparticles and their organic- and bioconjugates that form self-aggregates on a substrate.

Experimental Section

Synthesis of CdSe nanocrystals: CdO (4 mmol) and stearic acid (8 mmol) were mixed in ODE (5 mL) and heated to 250 °C under Ar to make a clear solution. After reducing the temperature below 130 °C, the solution volume was increased to 50 mL with ODE. Selenium powder (200-mesh, 2 mmol) was added and the temperature was raised to 240 °C at a rate of 25–30 °C min^{-1}. CdSe nanocrystals began to form at ~210 °C. The crystal growth was monitored by taking the absorption spectra. After reaching a steady state in growth, octylamine (5 mL) was injected to resume the growth. Red-emitting CdSe nanocrystals (λ_{abs} = 597 nm, λ_{em} = 611 nm) were purified several times with a solution of propylamine in methanol at room temperature and stored in hexane.

Synthesis of CdSe/ZnS nanocrystals: A zinc stock solution (50 mM) was prepared by mixing ZnO and oleic acid in ODE at ~240 °C. A sulfur stock solution (50 mM) was made by dissolving sulfur powder in ODE. The core solution was prepared by dispersing purified CdSe nanocrystals (0.1–0.3 μmol) in a mixture of ODE (2 mL) and ODA (4 g). After slowly heating up the core solution to 190 °C under Ar with vigorous stirring, the first monolayer portion of the zinc stock solution was swiftly injected into the core solution at once, followed by dropwise addition of the sulfur stock solution, and then the temperature was slowly raised to 190–210 °C over 5 min. Within 10 min, both zinc and sulfur stock solutions were alternately added dropwise for the next ML of ZnS shell. Final red-emitting CdSe/ZnS(3ML) nanocrystals (λ_{abs} = 606 nm, λ_{em} = 640 nm, 5.6 ± 0.4 nm TEM size) were harvested and washed with methanol.

Preparation of water-soluble nanocrystals: For the capping with MPA and MPO, CdSe/ZnS nanocrystals (20 mg) were dissolved in methanol (10 mL) containing ligand (100 μL). After adjusting pH to >10 with NMe_4OH, the mixture was stirred for 2 h at 60 °C under Ar. Water-soluble nanocrystals were precipitated with ethyl acetate (40 mL) and harvested by centrifugation (4000 rpm, 5 min). After washing twice with ethyl acetate, nanocrystals were dried under vacuum. For AET capping, CdSe/ZnS nanocrystals (20 mg) were dissolved in chloroform (10 mL), and mixed with AET hydrochloride (0.5 M, 200 μL) dissolved in methanol. The mixture was stirred for 6 h at 60 °C. Nanocrystal aggregates were washed with methanol and harvested by centrifugation (4000 rpm, 1 min). MPA-capped CdSe/ZnS (λ_{abs} = 600 nm, λ_{em} = 636 nm, FWHM 34 nm); MPO-capped CdSe/ZnS (λ_{abs} = 596 nm, λ_{em} = 634 nm, FWHM 35 nm); AET-capped CdSe/ZnS (λ_{abs} = 600 nm, λ_{em} = 637 nm, FWHM 34 nm).

DNA-conjugated nanocrsytals: MPA-capped nanocrystals (~1 nmol) were dissolved in PBS buffer (pH 7.4, 0.5 mL) and activated with 1-ethyl-3-[3-dimethylaminopropyl]carbodiimide hydrochloride (0.15 mg) and *N*-hydroxysulfosuccinimide (0.21 mg) at room temperature for 15 min. Thrombin-binding aptamer (5′-TTCACTGTGGTTGGTGTGGTTGG-3′) carrying a C_6-amine linker at the 5′ end was incubated with the activated nanocrystal solution and β-mercaptoethanol at room temperature for 2 h. The reaction was terminated with *N*-hydroxylamine hydrochloride.

TOF-SIMS analysis: The TOF-SIMS spectra were obtained with TOF-SIMS V (ION-TOF GmbH, Germany) equipped with a 25 keV Bi^+ ion gun. Experiments were repeated four times by preparing fresh sample every time. Each measurement yielded dissimilar micropatterns due to uncontrolled self-aggregation of nanocrystals on the substrate; however we arrived at the same conclusion regarding the conjugation of ligand. For TOF-SIMS imaging, the ion gun was operated at 5 kHz with 0.2 pA (Bi^+) average current at the sample holder. A bunch pulse of 0.7 ns duration resulted in mass resolution ($M/\Delta M$) > 8000. A 200×200 μm^2 area was rastered by primary ions to obtain the SIMS spectra while maintaining the ion dose below 10^{12} ions cm^{-2}. The negative ion mass spectra were internally calibrated using C^-, CH^-, C_2H^-, and C_4H^- peaks. All images presented in this work were taken in negative mode at 256×256 pixels with the spatial resolution of 1.5 μm.

FT-IR spectroscopy: The FT-IR spectra were taken with Nexus 6700 FT-IR (Thermo-Nicolet, Inc.) equipped with an attenuated total reflectance (ATR) accessory (Smart Miracle, PIKE Tech.). A drop of nanocrystal solution (~5 μL) was placed on a ZnSe-ATR crystal and dried under vacuum (1×10^{-2} torr) for 2 h. Mid-IR light was incident at 45° relative to the surface normal of crystal under N_2. The reflected light was detected by a liquid N_2-cooled HgCdTe detector. 300 scans were averaged to yield a spectrum at 2 cm^{-1} resolution.

Acknowledgements

We acknowledge the support from the Bio-Signal Analysis Technology Innovation Program of MOST/KOSEF, the R&D Program of Fusion Strategies for Advanced Technologies of MOCIE, POSTECH Biotech Center, Advanced Scientific Analysis Instruments Development Project (Grant No. RH0-2005-000-01004-0), and Korea Research Foundation (KRF-2006-005J01202).

Keywords: bioconjugation · mass spectrometry · nanocrystals · semiconductors · surface analysis

[1] a) X. Michalet, F. F. Pinaud, L. A. Bentolila, J. M. Tsay, S. Doose, J. J. Li, G. Sundaresan, A. M. Wu, S. S. Gambhir, S. Weiss, *Science* **2005**, *307*, 538–544; b) I. L. Medintz, H. T. Uyeda, E. R. Goldman, H. Mattoussi, *Nat. Mater.* **2005**, *4*, 435–446; c) J. M. Klostranec, W. C. W. Chan, *Adv. Mater.* **2006**, *18*, 1953–1964; d) S. K. Shin, H.-J. Yoon, Y. J. Jung, J. W. Park, *Curr. Opin. Chem. Biol.* **2006**, *10*, 423–429.

[2] F. Dubois, B. Mahler, B. Dubertret, E. Doris, C. Mioskowski, *J. Am. Chem. Soc.* **2007**, *129*, 482–483.

[3] a) W. Guo, J. J. Li, Y. A. Wang, X. Peng, *Chem. Mater.* **2003**, *15*, 3125–3133; b) F. Pinaud, D. King, H.-P. Moore, S. Weiss, *J. Am. Chem. Soc.* **2004**, *126*, 6115–6123.

[4] a) C. L. Brummel, I. N. W. Lee, Y. Zhou, S. J. Benkovic, N. Winograd, *Science* **1994**, *264*, 399–402; b) S. G. Ostrowski, C. T. van Bell, N. Winograd, A. G. Ewing, *Science* **2004**, *305*, 71–73; c) T. G. Lee, H. K. Shon, K.-B. Lee, J. Kim, I. S. Choi, D. W. Moon, *J. Vac. Sci. Technol. A* **2006**, *24*, 1203–1207; d) Y.-P. Kim, E. Oh, Y.-H. Oh, D. W. Moon, T. G. Lee, H.-S. Kim, *Angew. Chem.* **2007**, *119*, 6940–6943; *Angew. Chem. Int. Ed.* **2007**, *46*, 6816–6819.

[5] a) S. J. Lim, B. Chon, T. Joo, S. K. Shin, *J. Phys. Chem. C* **2008**, *112*, 1744–1747; b) Y. A. Yang, H. Wu, K. R. Williams, Y. C. Cao, *Angew. Chem.* **2005**, *117*, 6870–6873; *Angew. Chem. Int. Ed.* **2005**, *44*, 6712–6715.

[6] a) A. Michota, J. Bukowska, *J. Raman Spectrosc.* **2003**, *34*, 21–25; b) S. W. Han, S. W. Joo, T. H. Ha, Y. Kim, K. Kim, *J. Phys. Chem. B* **2000**, *104*, 11987–11995; c) S. Debrus, M. K. Marchewka, M. Drozd, H. Ratajczak, *Opt. Mater.* **2007**, *29*, 1058–1062.

[7] H. F. Arlinghaus, M. Ostrop, O. Friedrichs, J. Feldner, U. Gunst, D. Lipinsky. *Surf. Interf. Anal.* **2002**, *34*, 35–39.

[8] M. S. Akhter, *Colloids Surf. A* **1995**, *99*, 255–258.

Received: June 30, 2008
Published online: August 7, 2008

